Optical and elastic anomalies near the phase transition in $K_2Ge_8O_{17}$

1996 J. Phys.: Condens. Matter 8 4661

(http://iopscience.iop.org/0953-8984/8/25/020)

J. Phys.: Condens. Matter **8** (1996) 4661–4671. Printed in the UK

Optical and elastic anomalies near the phase transition in $K_2Ge_8O_{17}$

H-J Weber†, K Lüghausen‡, D Rheingans† and H Siegert‡

† Universität Dortmund, D-44221 Dortmund, Germany
‡ Universität zu Köln, D-50674 Köln, Germany

Received 5 February 1996, in final form 17 April 1996

Abstract. $K_2Ge_8O_{17}$ shows a structural phase transition near $T_c \approx 269$ K. The temperature dependence of the optical birefringence Δn, of the elastic stiffness constants c_{ij} and of the effective electro-optical coefficients $r_{(eff)}$ is determined. At T_c the derivative $\partial \Delta n/\partial T$ changes its sign. Elastic properties are studied by recording the acoustic resonances of a rectangular parallelepiped. We discuss those features of the method which are important in the investigation of phase transitions. No signature of elastic softening near T_c is observed in $K_2Ge_8O_{17}$. Below T_c, c_{44} and c_{66} increase continuously. The elastic hardening is accompanied by the onset of a small electro-optical effect. Its existence demonstrates the loss of the centre of symmetry, its anisotropy is consistent with a triclinic symmetry, and its magnitude suggests a spontaneous polarization of about 6×10^{-4} C m^{-2} in the low-temperature phase. Although $K_2Ge_8O_{17}$ is reminiscent of a weak ferroelectric material there are some observations which are uncommon to a paraelectric–ferroelectric phase transition.

1. Introduction

Several germanates show ferroelectric phase transitions but they cannot be regarded as typical ferroelectric materials. The truth of this statement becomes evident from a simple comparison of values for the spontaneous polarization $P_{(s)}$. Its magnitude in a typical ferroelectric oxide like $BaTiO_3$ or $LiNbO_3$ is $P_{(s)} = 0.4$ C m^{-2} [1]. This is significantly bigger than $P_{(s)} = 4 \times 10^{-2}$ C m^{-2} in $Pb_5Ge_3O_{11}$ [1] or $P_{(s)} = 1 \times 10^{-2}$ C m^{-2} in $LiNaGe_4O_9$ [2]. The values for $P_{(s)}$ are considered at about 40 K below T_c. A very small spontaneous polarization of 3×10^{-4} C m^{-2} is observed in $BaZnGeO_4$ [3] and in $Li_2Ge_7O_{15}$ (abbreviated as LGO) [4]. Equivalent to a small value of $P_{(s)}$ is a low Curie–Weiss constant or a weak polar soft mode. The chemical relationship between $K_2Ge_8O_{17}$ (abbreviated as KGO) and LGO is obvious. In addition the temperatures T_c are similar in the two crystals (269 K in KGO and 283 K in LGO [5]). Therefore one may expect similar mechanisms to be responsible for the phase transitions in the two crystals. LGO belongs to the class of so-called weak ferroelectrics. In these materials the critical divergence of the dielectric susceptibility at T_c is accompanied by the softening of some elastic constants [6]. The simultaneous appearance of dielectric and elastic anomalies indicates the mixing of optical and acoustical phonons. The structural feature which enables mode coupling is a nonvanishing component of internal strain [7, 8]. As in KGO forty parameters of this kind exist [9], mode coupling may happen very easily. Therefore it is important to study dielectric as well as elastic properties near the phase transition. In the present work we determine the changes in the elastic behaviour near T_c and we want to clarify whether a centre of

0953-8984/96/254661+11$19.50

symmetry still exists below T_c. Its absence is a necessary condition for a ferroelectric phase and consequently also for the possibility that KGO fits the scheme of weak ferroelectricity.

Among all of the alkali germanates, KGO is the compound with the smallest content of alkali oxide and it is the only compound without octahedral $GeO_{6/3}$ building units. In KGO, $GeO_{4/2}$ tetrahedra form rings in the (010) plane and chains along the *b*-axis. The space group is *Pnma* [10, 11]. The *b*-axis shows a pseudotetragonal symmetry which is reflected also by the optical and elastic properties [9]. Transformation heat and changes in the slope of the temperature dependence of the birefringence indicate a phase transition near 280 K [11]. Kizhaev *et al* [12] observed a B_{1g} mode in the Raman spectrum of KGO. It softens from 42 cm^{-1} at 1017 K to 17 cm^{-1} near T_c. Performing measurements of the dielectric constants with high accuracy in small temperature steps they detected a faint but well reproducible increase of ϵ_a and ϵ_c at the temperature $T_c = 269.6$ K. The weakness of the dielectric anomaly of 10^{-3} suggests that the trend in germanates towards weak ferroelectricity culminates in KGO.

The previous investigations of KGO demonstrate a weak influence of the phase transition on physical properties [11, 12]. Therefore we have selected sensitive experimental techniques to investigate changes near T_c. In section 2 we report the measurement of optical birefringence. Its dependence on temperature below T_c is believed to be proportional to the order parameter. Elastic measurements are presented in section 3. The elastic constants have been determined by recording the resonances of a rectangular parallelepiped. The theoretical background of this method of acoustic spectroscopy was developed two decades ago [13, 14], but its use in experiments dates back only to more recent work [15–19]. The method is believed to be an excellent probe of phase transitions [20] and has already been applied in this area [21, 22]. We consider its advantages and disadvantages for the investigation of elastic anomalies in some detail. The loss of the centre of symmetry is tested in section 4 by means of the linear electro-optical effect. In section 5 the essential features of the phase transition are summarized.

2. Birefringence

As already mentioned in section 1, different transition temperatures have been reported. The maximum in the dielectric constants occurs at $T_c = 269.6$ K [12]. Harbrecht, Kushauer and Weber [11] observed in different experiments and for different samples variations of the transition temperature between 275 K and 285 K. One reason for the variations can be a different quality of samples, because single crystals of KGO often show melt inclusions if the *b*-axis is the growth direction. To check such influences we determine the optical birefringence as a function of temperature for two samples. The thickness of sample S_1 is $L_1 = 0.39$ mm and it is cut from a bowl showing inclusions. Sample S_2 is optically clear and it is thicker than sample S_1 ($L_2 = 5.38$ mm). The light wave travels along [010] and the observed difference in refractive indices is $\Delta n = n_1 - n_3$. As shown in figure 1, Δn is the same in the two samples. We conclude that figure 1 shows a behaviour which is representative for KGO. Above 285 K the slope $\partial\,\Delta n/\partial T$ is constant which permits us to determine $\Delta n(T_c)$, which is the extrapolated value of Δn at the phase transition as shown in figure 1. Below T_c the quantity $\Delta n^* = \Delta n - \Delta n(T_c)$ is described by

$$\Delta n^* = C_{(b)}(T_c^{(b)} - T)^{1/2} \tag{1}$$

with $C_{(b)} = 75(\pm 5) \times 10^{-6}$ $K^{-1/2}$. $T_c^{(b)} = 268.2(\pm 0.9)$ K is the transition temperature determined by birefringence measurements. Equation (1) suggests that Δn^* is proportional to the order parameter Q and that the phase transition is of second order. Obviously there

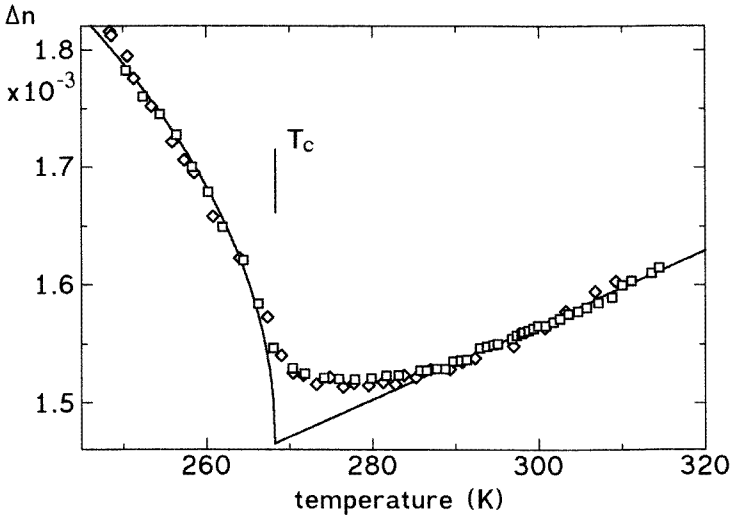

Figure 1. The optical birefringence $\Delta n = n_1 - n_3$ in the vicinity of the phase transition of $K_2Ge_8O_{17}$. Results are shown for the two samples S_1 (open diamonds) and S_2 (full squares) described in the text. Solid lines are fits as explained in the text.

exists an intermediate range $T_c < T < 290$ K with a nearly constant birefringence. A comparison of the KGO lattice constants at 123 K, 293 K, and 523 K [11] shows that thermal expansion is nearly the same above and below T_c whereas $\partial \Delta n/\partial T$ changes its sign at T_c. We conclude that no significant spontaneous strain is connected with the phase transition.

Due to the intermediate range, the determination of a unique value for T_c is difficult. Therefore we believe that $T_c^{(b)} = 268.2$ K is not necessarily inconsistent with $T_c = 269.6$ K which is the maximum of the dielectric constant [12]. For both samples, S_1 and S_2, we are unable to detect a rotation of the optical indicatrix which apparently contradicts an earlier observation [11]. We would like to mention that figure 1 is reminiscent of the phase transition in LGO where the difference $n_3 - n_1$ shows qualitatively the same dependence on temperature [23].

3. Elastic measurements

In our apparatus for acoustic spectroscopy the sample is mounted between two piezoelectric transducers. The first transducer excites the sample and the second transducer detects its vibrations while the frequency is scanned [22, 19]. Figure 2 shows a small part of the spectrum at two temperatures. The shifts of the resonance frequencies f_m are a consequence of the phase transition occurring between the two temperatures. Obviously, the shifts can be determined with a high sensitivity. We observe a high accuracy, too. On remounting the sample in the cryostat and repeating the temperature run, the resonance frequencies at a specific temperature are reproduced with a relative error of less than 4×10^{-4}. The narrowness of the peaks indicates a sample of high quality. In figure 2 f_1, f_2, and f_3 are presented. We analysed more than fifty resonances. This is a sufficient number of data for determining all nine elastic constants of an orthorhombic crystal in one run and for one sample.

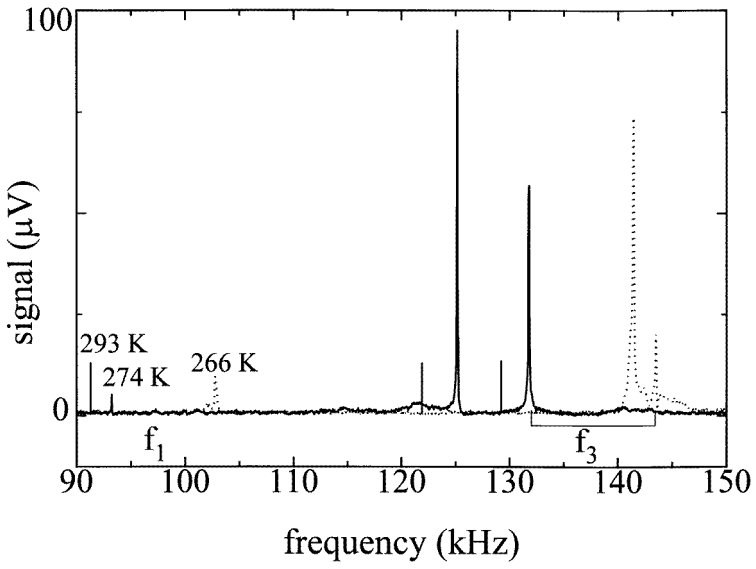

Figure 2. A small part of the acoustic spectrum for 274 K (solid line) and 266 K (broken line). For the sake of comparison the positions of the three resonances f_1, f_2 (unmarked peaks), and f_3 are shown for 293 K, too. Notice the comparatively small frequency shifts above the phase transition occurring at 269 K.

The ease and the accuracy of the experimental procedure is 'paid for' by the large amount of numerical calculation needed for analysing the spectrum [16, 20]. Besides this technical problem, the method shows a more intrinsic disadvantage, too. In most resonance frequencies the contribution of the elastic constants c_{44}, c_{55}, and c_{66} is dominant and they can be determined with high accuracy. This is not the case with the other coefficients. Another problem is the assignment of modes if they are close together. This may easily become the case in the course of a phase transition because different modes show a different dependence on temperature. As a consequence crossing of modes and frequency shifts due to a repulsion of coupled resonances can be observed. Furthermore the disappearance of a resonance due to the temperature dependence of its oscillator strength is possible. For these reasons it is important to inspect the variation of each resonance frequency carefully in the course of a phase transition.

Table 1. Elastic constants c_{ij} (unit: GPa) of $K_2Ge_8O_{17}$ at 293 K. Uncertainties are given in parentheses.

$c_{11} = 65.9(0.7)$	$c_{12} = 26(1)$	$c_{44} = 4.8(0.1)$
$c_{22} = 87.3(1.0)$	$c_{13} = 9(1)$	$c_{55} = 20.6(0.1)$
$c_{33} = 56.2(0.4)$	$c_{23} = 19(1)$	$c_{66} = 12.8(0.1)$

We proceed in the following way. At ambient temperature the resonance data are verified by measuring the velocity of ultrasonic waves. In this way ambiguity in the assignment of some modes is removed. The result is the set of elastic constants shown in table 1. The elastic constants and all other tensor quantities used in the present paper are referred to a system of Cartesian coordinates with its axes parallel to the orthorhombic axes of the

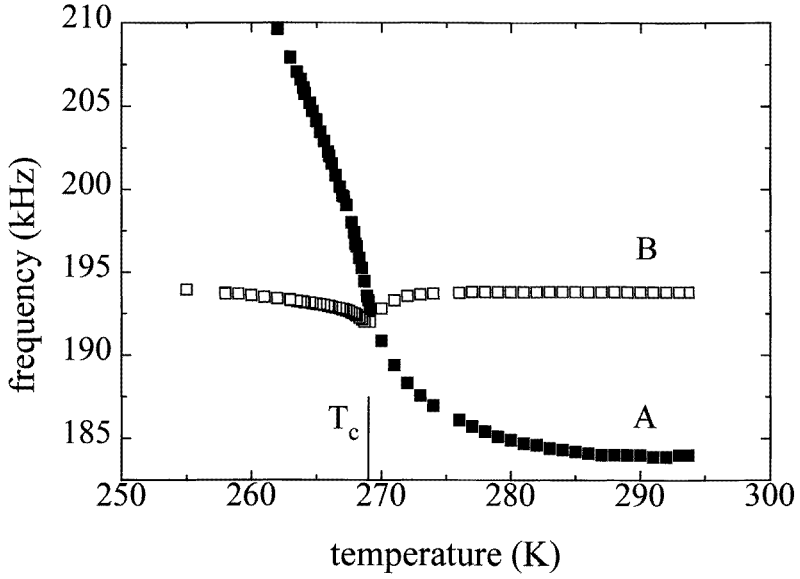

Figure 3. The resonance frequency of two selected modes versus temperature.

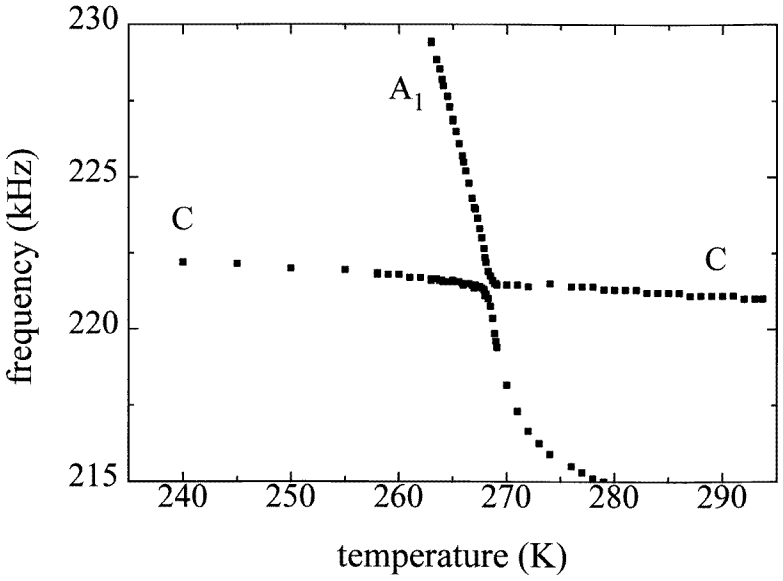

Figure 4. The resonance frequency of two selected modes versus temperature. Notice the constant slope of mode 'C'.

crystal. The basic features of the elastic behaviour near T_c are demonstrated in figures 3 and 4. Figure 3 exhibits $f_m(T)$ for two different modes. Near room temperature $\partial f_m/\partial T$ is very small. On decreasing the temperature, the dependence on T is stronger for mode

'A' than for mode 'B'. The behaviour of mode 'A' is characterized by

$$\frac{\partial f_m^A}{\partial T} < 0 \qquad \text{with} \begin{cases} \dfrac{\partial^2 f_m^A}{\partial T^2} > 0 & \text{for } T > T_c \\ \dfrac{\partial^2 f_m^A}{\partial T^2} < 0 & \text{for } T < T_c. \end{cases}$$

For mode 'B' we observe

$$\frac{\partial f_m^B}{\partial T} > 0 \qquad \text{for } T > T_c$$
$$\frac{\partial f_m^B}{\partial T} < 0 \qquad \text{for } T < T_c.$$

About 70% and 30% of all resonances show a dependence on temperature like mode 'A' and mode 'B', respectively. There is one exception, and that is the curve denoted by 'C' in figure 4. It is characterized by a linear dependence on T over the whole range of temperatures under investigation. The crossing of 'C' and 'A_1' in figure 4 is a nice example of repulsion due to mode coupling.

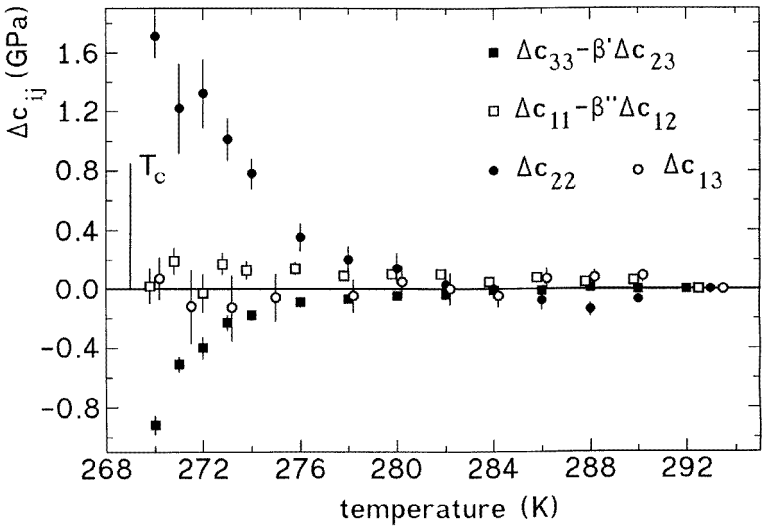

Figure 5. The temperature dependence of some elastic constants above T_c.

Above T_c the changes of the resonance frequencies are rather small. This permits us to determine the changes of the elastic constants by considering the linear relationships

$$\Delta f_m = \sum_{i,j} \frac{\partial f_m}{\partial c_{ij}} \Delta c_{ij}.$$

Here $\Delta f_m = f_m(T) - f_m(293\ \text{K})$ and $\Delta c_{ij} = c_{ij}(T) - c_{ij}(293\ \text{K})$ are the increments of f_m and c_{ij} in the temperature range $T_c \leqslant T \leqslant 293$ K. The derivatives $\partial f_m/\partial c_{ij}$ are calculated by use of the elastic constants given in table 1. The numerical values show that $\partial c_{55}/\partial T$ is responsible for the constant value of $\partial f_m^C/\partial T$. Thus the phase transition has no impact of on c_{55}. Furthermore the strong changes of mode 'A' resonance frequencies are caused by $\partial c_{44}/\partial T$ and $\partial c_{66}/\partial T$. The influence of the phase transition on modes 'B'

occurs only in the close vicinity of T_c. In these modes mainly the elastic constants c_{ij} with $i, j \leqslant 3$ are involved. A comparison of the derivatives $\partial f_m^A/\partial c_{44}$ and $\partial f_m^A/\partial c_{66}$ with $\partial f_m^B/\partial c_{ij}$ $(i, j \leqslant 3)$ shows that the latter quantities are usually smaller by a factor of ten. This renders an exact determination of $\partial c_{ij}/\partial T$ with $i, j \leqslant 3$ more difficult than of $\partial c_{44}/\partial T$ and $\partial c_{66}/\partial T$. The problem is aggravated by two approximately linear dependences which can be described by the increments

$$\Delta c^* = \Delta c_{11} - \beta^* \Delta c_{12} \qquad \text{and} \qquad \Delta c^{**} = \Delta c_{33} - \beta^{**} \Delta c_{23}.$$

To obtain the best result we proceed in the following way. There are a sufficient number of resonances (14) with a negligible contribution of Δc_{44}, Δc_{55} and Δc_{66} and with nearly equal values for β^* and β^{**}, respectively. Selecting these resonances, the changes Δc^*, Δc^{**}, Δc_{22}, and Δc_{13} can be determined with a higher accuracy than all changes Δc_{ij} even if they are deduced from a large number of modes (50). Results for $T > T_c$ are presented in figure 5. They show that

$$\frac{\partial c_{11}}{\partial T} = \frac{\partial c_{12}}{\partial T} = \frac{\partial c_{13}}{\partial T} = 0. \tag{2}$$

Approaching T_c from room temperature, c_{22} becomes harder and only c^{**} decreases slightly. The analysis with all of the elastic constants and with all of the modes shows that this decrease is caused by a hardening of c_{23} rather than by a softening of c_{33}.

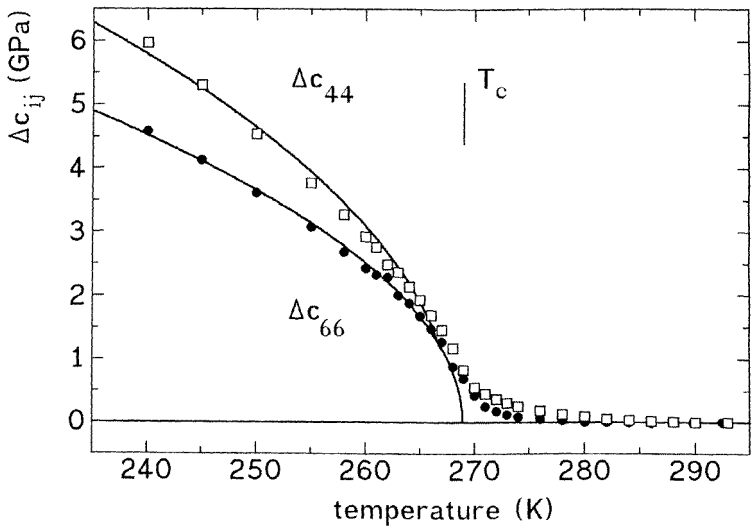

Figure 6. Elastic constants c_{44} and c_{66} versus temperature.

We are not able to establish any elastic softening near T_c. Thus the small values of c_{44} and c_{13} observed at room temperature (see table 1) are not precursors of the phase transition.

Below T_c least-squares fits on the basis of an orthorhombic symmetry yield acceptable results only for c_{kk} with $k = 4, 5, 6$. The constant value for $\partial c_{55}/\partial T$ has already been mentioned above. As shown in figure 6, c_{44} and c_{66} change continuously at T_c. Below T_c their dependence on temperature is described by

$$c_{ij} = c_{ij}^0 + C_{(el)}(T_c^{(el)} - T)^{1/2} \tag{3}$$

where c_{ij}^0 is the value at 293 K. The transition temperature is $T_c^{(el)} = 269(\pm 1)$ K. As demonstrated in figure 6 and also in figure 3 by mode 'A', $\delta c_{44}/\delta T \neq 0$ and $\delta c_{66}/\delta T \neq 0$ is already observed below 285 K. Thus, the two elastic constants show a similar intermediate range to the birefringence in figure 1. In both cases the intermediate range is most probably caused by fluctuations of the order parameter.

4. Electro-optic measurements

The onset of ferroelectricity is inevitably connected with the loss of the centre of symmetry. This can be tested very sensitively by measuring the linear electro-optical effect which describes the impact of an electric field on the relative dielectric impermeability tensor a_{ij} via

$$\Delta a_{ij} = r_{ijk} E_k. \tag{4}$$

Measurements are performed on three samples of different dimensions but with the same orientation. All edges are parallel to the crystallographic axes. We chose the transversal configuration with the electric field $\boldsymbol{E}$ perpendicular to the wavevector. The light source is a He–Ne laser. Using alternating fields and a lock-in detection system, the induced changes in the optical birefringence are recorded with high sensitivity. We do not determine the absolute sign of the electro-optical effects.

Table 2. The linear electro-optical effect in $K_2Ge_8O_{17}$. The temperature dependence of the coefficients r_{ijk} is described by equation (5). The fitting parameters are $C_{(r)}$ (unit: 10^{-14} mV^{-1} K$^{-1/2}$) and $T_c^{(r)}$ (unit: K). $T_c^{(b)}$ is determined by measuring optical birefringence. Numbers with and without an asterisk denote data taken on warming and on cooling, respectively. Rows marked by the same number belong to measurements with the same orientation of the electric field $\boldsymbol{E}$ and of the wavevector $\boldsymbol{k}$. S_3, S_4, and S_5 represent three different samples.

No	$\boldsymbol{E}$	$\boldsymbol{k}$	$r_{iii} - r_{jji}$	Sample	C_r	$T_c^{(r)}$	$T_c^{(b)}$
1a	[100]	[010]	$r_{111} - r_{331}$	S_3	0.184(6)	264.5(3)	
1b*				S_3	0.210(25)	268.4(3)	
2	[100]	[001]	$r_{111} - r_{221}$	S_4	−0.229(7)	266.3(3)	
3	[010]	[100]	$r_{222} - r_{332}$	S_3	0.012(2)	263.6(9)	
4	[001]	[100]	$r_{333} - r_{223}$	S_3	0.211(9)	264.3(4)	
5a	[010]	[001]	$r_{222} - r_{112}$	S_4	0.318(9)	266.5(4)	
5b*				S_5	0.206(8)	267.8(8)	
6a*	[001]	[010]	$r_{333} - r_{113}$	S_5	−0.285(9)	266.8(3)	268.2(5)
6b*				S_5	−0.369(24)	267.9(9)	268.2(5)
6c*				S_5	−0.646(22)	268.7(4)	268.2(4)
6d				S_5	−0.642(55)	266.7(6)	268.2(4)

A typical result is presented in figure 7. It is obtained by decreasing the temperature step by step and determining the electric-field-induced birefringence at constant T. Below T_c a small linear electro-optical coefficient of about 10^{-15} m V^{-1} is observed (squares in figure 7). This is significantly smaller than the effect in α-quartz ($r_{111} = 4 \times 10^{-13}$ m V^{-1}) or in KDP ($r_{123} = 10^{-11}$ m V^{-1}). In a second run the sample is cooled step by step under

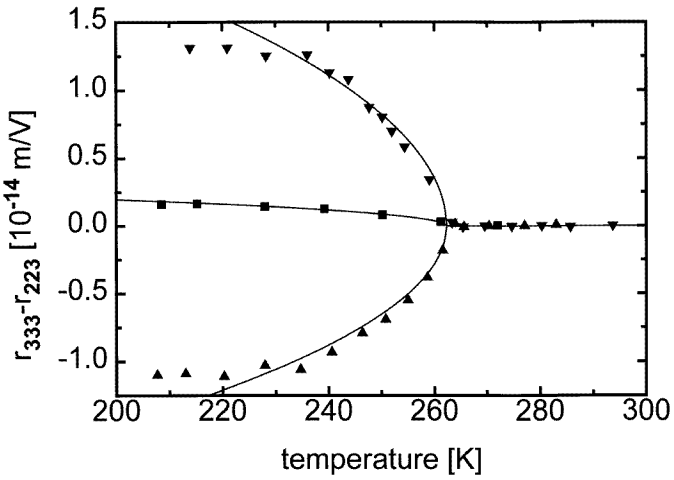

Figure 7. The electro-optical coefficient $r_{333} - r_{223}$ of KGO for cooling runs with different static fields E_{dc}. □: $E_{dc} = 0$; ▲: $E_{dc} > 0$; ▼: $E_{dc} < 0$. Solid lines show fits made using equation (5).

the action of a static electric field. At constant temperatures the dc field is switched off only for the time which is needed to measure the electro-optical effect with alternating fields. Now the coefficients $r_{333} - r_{223}$ are bigger than in the first run. They change sign in a third temperature run with the opposite direction of the dc field. The influence of the dc field is easily explained by the existence of a spontaneous polarization with a component along the crystallographic *c*-axis. On cooling the sample without an external dc field, domains with both orientations of $P_{(s)}$ are created below T_c. By the action of a dc field it becomes homogeneously polarized. In the vicinity of the transition temperature the effective electro-optical coefficient is described by

$$r_{(eff)} = C_{(r)}(T_c^{(r)} - T)^{1/2} \tag{5}$$

where $r_{(eff)}$ represents the difference of two coefficients r_{ijk} and contains piezoelectric contributions. The experiment shown in figure 7 was repeated for different orientations. It turned out that in all measurements equation (5) works well from $T_c^{(r)}$ to about $T_c^{(r)} - T = 20$ K. At low temperatures $r_{(eff)}(T)$ differed significantly from the temperature dependence given by equation (5). Nevertheless equation (5) represents an appropriate relation for use in comparing the magnitude of the effect and the transition temperature observed in different measurements. The results of least-squares fits are summarized in table 2. All of the values were obtained from runs in which the sample was cooled under the action of a static electric field. The data were recorded on cooling or on warming.

First we discuss the order of magnitude observed for $r_{(eff)}$. Assuming a spontaneous polarization $P_{(s)}$ as the origin of the linear electro-optical effect, equation (4) can be written as

$$\Delta a_{ij} = \epsilon_0 M_{ijmn} \chi_{nk} P_{(s)m} E_k \tag{6}$$

where χ_{ij} is the relative static susceptibility. From Miller's rule [24] the coefficient M_{ijkl} of the quadratic electro-optical effect varies smoothly in different materials. Inspecting the experimental data reported for 26 different crystals we obtain the average value $\bar{M} = 0.21(\pm 0.07)$ m^4 C^{-2}. Using average values also for r_{ijk} (see table 2) and χ_{ij} [12]

for KGO we are able to estimate $P_{(s)}$ as shown by a comparison of equation (6) with equation (4). The result is

$$P_{(s)} = 6 \times 10^{-4} \text{ C m}^{-2}. \tag{7}$$

This is of the same order of magnitude as observed for the germanate $Li_2Ge_7O_{15}$ [4].

The observed value for $r_{222} - r_{332}$ (table 2) is so small that it may be due to a misorientation of the sample. $r_{222} - r_{332} = 0$ is consistent with a mirror plane perpendicular to the *b*-axis which again is consistent with the observed anomaly of the dielectric constants [12]. However, this interpretation is made inadmissible by the comparatively large values for $r_{222} - r_{112}$ (table 2) obtained for two different samples. Taking into account that for all configurations in table 2 the linear electro-optical effect exists, we conclude that there is a triclinic symmetry below T_c.

Table 2 demonstrates several unusual features of the electro-optical effect. Its magnitude and the temperature $T_c^{(r)}$ depend on experimental conditions. Measurements Nos 5a and 5b show different $C_{(r)}$ for two different samples. In general $T_c^{(r)}$ is smaller for measurements on cooling than on warming which is inconsistent with the continuous onset of the effect below T_c. The position of the light beam in the sample varies in experiments 6a, 6b, and 6c. Obviously the sample is inhomogeneous with respect to the electro-optical effect. The variation of $C_{(r)}$ is no experimental mistake as demonstrated by the combined measurements 6c/6d and 1a/1b. In both cases the laser position in the sample was the same and the values for $C_{(r)}$ agreed within the experimental accuracy in the two temperature runs. In all No 6 measurements, optical birefringence was determined simultaneously with the electro-optical effect. As the values for $T_c^{(b)}$ coincide in all of the runs, the variation of the transition temperature is restricted to the electro-optical effect. This suggests the following simple explanation for the observed variations. Due to the low symmetry the domain structure below T_c is rather complex. In addition the linear electro-optical effect is small. Thus an unusually strong influence of crystal imperfections on the measurements is possible.

5. Conclusion

The temperature dependence of Δn^* (equation (1)), Δc_{44} and Δc_{66} (equation (3)), and $r_{(eff)}$ (equation (5)) suggests that these quantities are coupled to the order parameter Q below T_c. The nature of Q cannot be clarified decisively by the present experiments. However, we are able to exclude the possibility that a spontaneous strain is the intrinsic order parameter. The existence of a small electro-optical effect below T_c is consistent with the assumption of a weak ferroelectric phase. In this case the order parameter is the spontaneous polarization $P_{(s)}$, but in contrast to the case of a common ferroelectric phase, $P_{(s)}$ should change its sign at low temperatures [25]. In LGO the typical feature of a change of sign has been demonstrated for different properties depending on $P_{(s)}$ [26]. We have checked the possibility of such a behaviour in KGO by measuring $r_{333} - r_{223}$ and $r_{111} - r_{331}$ for an extended temperature range. In both cases we do indeed observe a strong decrease of the effect at low temperatures but no change in the sign. Thus KGO follows the general scheme of a weak ferroelectric material but it is an untypical example.

References

[1] Nomura S, Adachi M, Harada J, Ikeda T, Sawaguchi E and Yamada T 1981 *Landolt–Börnstein New Series* vol III/16, ed K-H Hellwege and A M Hellwege (Berlin: Springer) pp 334, 491, 577

[2] Wada M, Shibata M, Sawada A and Ishibashi Y 1983 *J. Phys. Soc. Japan* **52** 2981

[3] Tanba N, Wada M and Ishibashi Y 1985 *J. Phys. Soc. Japan* **54** 4783
[4] Wada M and Ishibashi Y 1983 *J. Phys. Soc. Japan* **52** 193
[5] Haussühl S, Wallrafen F, Recker K and Eckstein J 1980 *Z. Kristallogr.* **153** 329
[6] Siny I 1993 *Ferroelectrics* **150** 119
[7] Dvořák V 1968 *Phys. Rev.* **167** 525
[8] Unoki H 1995 *J. Phys. Soc. Japan* **64** 1579
[9] Weber H-J 1995 *Phys. Rev.* B **51** 12 209
[10] Fay E, Völlenkle H and Wittmann A 1973 *Z. Kristallogr.* **138** 439
[11] Harbrecht B, Kushauer J and Weber H-J 1990 *Eur. J. Solid State Inorg. Chem.* **27** 831
[12] Kizhaev S, Pisarev R, Farhi R and Weber H-J 1995 *Ferroelectrics* **170** 215
[13] Demarest H 1971 *J. Acoust. Soc. Am.* **49** 768
[14] Ohno I 1976 *J. Phys. Earth* **24** 355
[15] Yamamoto S, Ohno I and Anderson O 1988 *J. Phys. Chem. Solids* **48** 143
[16] Yasuda H and Koiwa M 1991 *J. Phys. Chem. Solids* **52** 723
[17] Lei M, Sarrao J, Visscher W, Bell T, Thompson J, Migliori A, Welp U and Veal B 1993 *Phys. Rev.* B **47** 6154
[18] Willis F, Leisure R and Jacob I 1994 *Phys. Rev.* B **50** 13 792
[19] Weber H-J, Lüghausen K, Haselhoff M and Siegert H 1995 *Phys. Status Solidi* b **191** 105
[20] Maynard J 1996 *Phys. Today* **26**
[21] Migliori A, Visscher W, Wong S, Brown S, Tanaka I and Allen P 1990 *Phys. Rev. Lett.* **64** 2458
[22] Lüghausen K, Siegert H, Woike T and Haussühl S 1995 *J. Phys. Chem. Solids* **56** 1291
[23] Kaminski W 1989 *Doctoral Thesis* Universität zu Köln
[24] Miller R 1964 *Appl. Phys. Lett.* **1** 17
[25] Tagantsev A 1987 *JETP Lett.* **45** 447
[26] Bush A and Venevtsev Y 1986 *Sov. Phys.–Solid State* **28** 1101